Hyper-Raman-active soft mode in $Pb(Mg_{1/3}Nb_{2/3})_{0.73}Ti_{0.27}O_3$

Holger Hellwig*
Department of Geology, University of Illinois at Urbana-Champaign, 1301 West Green Street, Urbana, Illinois 61801, USA

Alp Sehirlioglu and David A. Payne
Department of Materials Science and Engineering and Frederick Seitz Materials Research Laboratory, University of Illinois at Urbana-Champaign, Urbana, Illinois 61801, USA

Pengdi Han
H. C. Materials Corporation, Urbana, Illinois 61802, USA
(Received 16 December 2005; published 28 March 2006)

Hyper-Raman measurements on $Pb(Mg_{1/3}Nb_{2/3})_{0.73}Ti_{0.27}O_3$ (PMN-27%PT) in a temperature range between 513 K and 873 K revealed the existence of two vibrational modes below 50 cm^{-1} and a central peak. Both modes soften with decreasing temperature. The squared frequency of the lower frequency mode shows linear temperature dependence and approaches zero at 571 K. This mode has been assigned T_{2u} symmetry. Its displacements only involve lead-oxygen bonds and do not affect the dielectric behavior. The higher frequency mode has been assigned T_{1u} symmetry and is responsible for the ferroelectric phase transition in pure lead titanate. Below 570 K this mode strongly couples to the central peak and shows a pronounced nonlinear decrease in the vibrational frequencies and increase in mode strength with decreasing temperature. The central peak is the dominant feature in the vibrational spectrum below 570 K. The critical behavior is supported by the temperature dependence of the mode coupling parameters, the central peak, and the hyper-Rayleigh peak.

DOI: 10.1103/PhysRevB.73.094126 PACS number(s): 77.84.Dy, 63.20.Dj, 64.60.Ht, 78.30.−j

I. INTRODUCTION

Relaxor-based materials show outstandingly high electrostrictive coupling and are therefore used as actuators and positioners. They are characterized by a frequency dependent temperature of the maximum of the dielectric constant in combination with a diffuse, ferroelectric phase transition. Despite strong efforts, a comprehensive picture and understanding of relaxor materials has not been achieved, yet. An important group of relaxor materials are lead based solid solutions, including $(1-x)PbMg_{1/3}Nb_{2/3}O_3-xPbTiO_3$ (PMN-xPT). The phase diagram of PMN-xPT shows a morphotropic phase boundary (MPB) which divides the ferroelectric low temperature phase of the PT rich side from the low temperature phase of the PMN rich component.[1] PT crystallizes in the perovskite structure and undergoes a phase transition at 766 K from a high temperature cubic phase (space group $Pm\bar{3}m$, $Z=1$) to a low temperature tetragonal phase (space group $P4mm$, $Z=1$),[2] characterized by a ferroelectric soft-mode.[3–5] Pure PMN has cubic symmetry. With increasing PT content a slight rhombohedral distortion was found,[6,7] while close to the MPB other symmetries have been reported as well.[8–10] Close to the MPB a strong dependence of the thermal properties on domain orientations and poling history was observed as well.[11] Inelastic neutron studies revealed the existence of low frequency resonances and observed mode coupling, but lack of higher resolution at low energies puts limitations on the interpretations.[12–15]

II. EXPERIMENTAL PROCEDURE

We carried out hyper-Raman measurements[16] on a single crystal of PMN-27%PT in a temperature range of 513–873 K in the cubic phase, well above the stability of the low temperature phase. The specimen was a plate of dimensions $5\times5\times1$ mm^3 with faces parallel cubic {100}. It was placed in a hot stage and temperature stabilized within ±2 K. Heating and cooling rates were less than 2 K/min and all data were collected with decreasing temperature on unpoled samples. Hyper-Raman spectra were collected in 160° backscattering geometry with less than 600 mW of incident total laser power (pulsed neodymium-yttrium vanadate laser operating at a wavelength of 1064 nm, 30 kHz repetition rate, 15 ns pulse width, focused with a lens of focal length $f=150$ mm to a spot size of 25 μm). Scattered light was collected by a microscope objective with numerical aperture NA=0.23 and a 0.5 m spectrometer with a liquid nitrogen cooled CCD camera. At each temperature, spectra with two different gratings, 600 and 1800 grooves per mm, were collected resulting in resolutions of about 3 cm^{-1} and 1 cm^{-1}, respectively, based on the width of the hyper-Rayleigh peak. These spectra will be referred to as low (3 cm^{-1}) and high (1 cm^{-1}) resolution spectra. Each spectrum was collected for 600 s and 8–20 spectra were finally averaged and corrected for cosmic rays (except for high resolution spectra taken at 513, 573, and 673 K, which were averaged over 60–90 single measurements). Further experimental details can be found elsewhere.[17] A full spectrum fit was applied to the averaged data.[18] In general, we tried to keep the number of free parameters as small as possible, judged by the sum of squared residuals. The results therefore represent the lowest number of free parameters needed in order to reproduce the measured spectra within a statiscally meaningful range. Each spectrum is described by a constant background and a Gaussian hyper-Rayleigh peak. At temperatures above 673 K a thermal background (Planck spectrum) with one additional

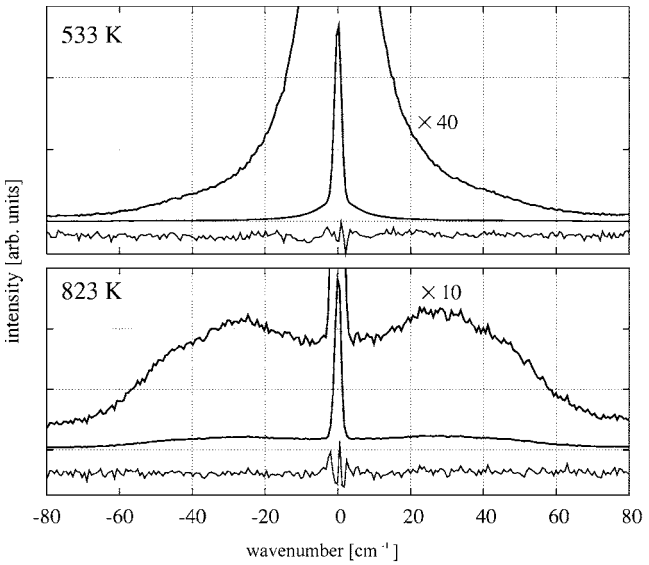

FIG. 1. Hyper-Raman spectrum of PMN-28%PT at 533 K and 823 K showing details in the low frequency region. For each temperature, the upper two curves represent measured data in different magnifications and the lower curves show the residuals divided by the square root of the background substracted intensity, offset and multiplied by a factor of 1000 (533 K) and 100 (823 K) for clarity.

parameter (scaling factor) was added. Details about the high frequency range above 100 cm^{-1} will be presented elsewhere. Every spectrum was found to be stable within the local parameter space. Starting parameters were derived from fitted spectra at similar temperatures. Additionally, starting parameters were changed to check for robustness. All spectra were corrected by a thermal occupation factor $n(\omega)+1$ with $n(\omega)=1/(\exp(\hbar\omega/kT)-1)$.

III. RESULTS AND DISCUSSION

In the frequency range below 100 cm^{-1} spectra at different temperatures differ significantly (Fig. 1). At temperatures above 773 K two doublets can be resolved in the low frequency part of the spectrum (at low frequencies the Stokes- and anti-Stokes components appear as doublets symmetrically spaced around the zero reference line of the hyper-Rayleigh peak) (lower part in Fig. 1). Attempts to fit this region with only one resonance and/or a central peak does not accurately describe the measured data. At lower temperatures this region shows strong characteristics of a central peak (upper part in Fig. 1). Attempts to fit the spectra using two resonances and an additional central peak were only partially successful and revealed persistent excess intensity of the calculated spectra in the frequency range around 70 cm^{-1}. Reduced intensities in vibrational spectra are often the hallmark of mode coupling,[18] a phenomenon commonly observed in PMN-PT.[12–15] With one more additional fitting parameter describing imaginary coupling between the central peak and the higher frequency resonance of the two modes below 100 cm^{-1} (Ref. 19) a satisfactory fit was achieved at all temperatures. At temperatures below 513 K low frequency data are not available because of the strong increase in intensity of the hyper-Rayleigh peak.

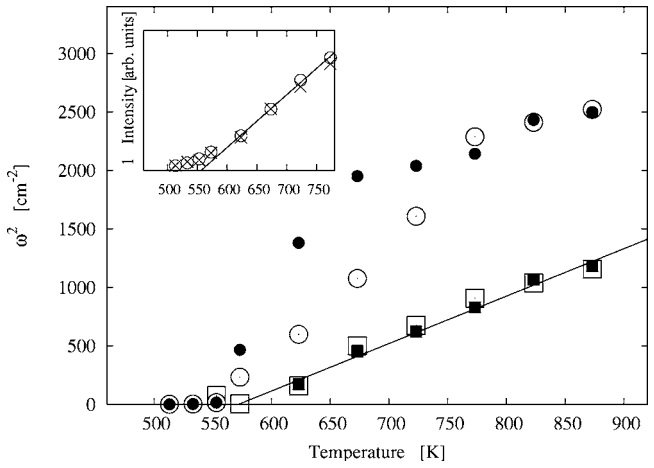

FIG. 2. Temperature dependence of squared frequencies of the low frequency modes of PMN-28%PT. Squares: uncoupled mode together with a linear fit (line), circles: coupled mode [filled (open) symbols: high (low) resolution data]. Error bars for the high resolution data are given where the error exceeds the size of the symbol. Inset: Temperature dependence of inverse intensity of hyper-Rayleigh peak with linear fit above 600 K [circles (crosses): high (low) resolution data].

In Fig. 2 the squared frequencies of the low frequency modes are shown for both high and low resolution data. The uncoupled lower frequency mode shows good agreement between both data sets. At temperatures below 573 K (553 K) the high (low) resolution spectra could equally well be fitted without this resonance. The squared frequencies of this lower frequency mode were fitted to a straight line, which intersects the zero line at 571 K ± 10 K (Fig. 2). The linear temperature dependence of the squared frequencies indicates classical soft-mode behavior with a phase transition at 571 K. The other low frequency mode at higher frequencies shows less consistent behavior between the two data sets, due to larger uncertainties of the fitted parameters based on mode coupling with the central peak. With the relatively wider linewidth of the hyper-Rayleigh peak and the smaller number of data points in the low resolution data sets we believe that results from the high resolution data sets (full symbols in Fig. 2) are more trustworthy. Despite these uncertainties the mode frequencies of this mode clearly drop to zero at temperatures below 571 K and a simple linear temperature dependence above 571 K cannot be observed. Coupling strongly increases with decreasing temperature and the inverse coupling constant $1/\Gamma$ shows nearly linear temperature dependence as well, intersecting the zero line at 542 K ± 15 K (see inset in Fig. 3). The intensity and the relaxation time τ (defined as the inverse peak width of the central peak) shows a maximum in the temperature region where the frequencies of the low frequency modes approach zero, supporting the notion of critical behavior in this temperature range (Fig. 3). We also measured the dielectric constant on the same sample. The inverse dielectric constant shows a deviation from a linear trend at higher temperatures (Curie-Weiss Law) around 571 K. No maximum or excess in

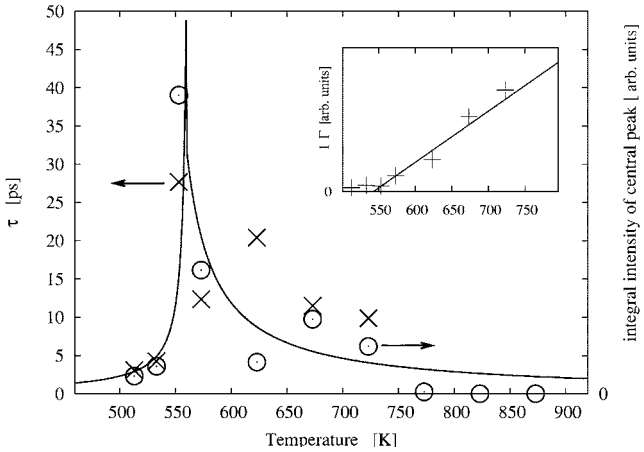

FIG. 3. Temperature dependence of the integral intensity (circles) and the width (crosses) of the hyper-Raman active central peak of PMN-28%PT (lines are to guide the eye). Inset: temperature of inverse coupling constant with linear fit.

the inverse dielectric constant was observed at this temperature. The temperature of 571 K also coincides with the beginning of a deviation from a linear behavior of the optical index of refraction in PMN,[20] and of the cubic lattice constants in PMN (Ref. 21) and in PMN-PT (Ref. 8) and is usually referred to as the Burns temperature T_d.[20] The relatively low intensity of the hyper-Rayleigh peak at 600 K and above clearly indicates that the high temperature phase is centrosymmetric. The temperature dependence of the intensity of the hyper-Rayleigh peak can also be used as a measure for structural precursors associated with a phase transition.[22,23] Plotting the inverse intensity against temperature shows a linear behavior above 600 K which extrapolates to zero at 556 K±15 K (552 K±20 K for the low resolution data) (see inset in Fig. 2).

In order to assign mode symmetries to the low frequency modes we will discuss possible high temperature structures for PMN-PT. Because of possible ordering of the B-site a $2\times2\times2$ superstructure provides partial ordering for the Mg and Nb atoms,[24] where one sublattice is occupied by only Nb atoms and the other sublattice contains the remaining Nb and Mg atoms, leading to space group $Fm\bar{3}m$. Note that this ordering scheme provides the lowest energy with respect to electrostatic interactions between the B-site cations of different charge. Doubling of the unit cell in our sample has been confirmed by x-ray analysis. In $Fm\bar{3}m$ the hyper-Raman active vibrational modes include four IR active T_{1u} and one only hyper-Raman active T_{2u} mode, while the simple cubic perovskite structure (space group $Pm\bar{3}m$) also shows one only hyper-Raman active T_{2u} mode, but only three IR active T_{1u} modes. As three-dimensional representations, T_{2u} and T_{1u} can have different orientations, resulting in tetragonal or rhombohedral symmetry if oriented along (001) or (111), respectively. The transverse ferroelectric T_{1u} soft-mode is described by a coherent motion of the oxygen framework against the cations with displacement vectors along the orientation of T_{1u}. The actual magnitude of the displacements of the Pb and the B-site atoms depends on the interatomic potentials. The vibrational mode pattern of the T_{2u} mode does not involve any displacement of cations; only the oxygen ions are moving within the plane perpendicular to the fourfold axis of its tetragonal site symmetry. This plane contains the lead ions and the oxygen displacement has only small components along the oxygen-B-site bond. The specific displacement within this plane is given by the direction of the T_{2u} mode. For T_{2u} along (111) the displacement of the oxygen ions is directly along the oxygen-lead bond. Within the (111) plane three of the six oxygens surrounding one lead ion move closer and three move further away. The three oxygens above and below that plane rotate clockwise and counterclockwise, respectively (see Fig. 4). The displacement of the oxygens located at $0,\frac{1}{2},\frac{1}{2}$, at $\frac{1}{2},0,\frac{1}{2}$, and at $\frac{1}{2},\frac{1}{2},0$ (in a unit cell without superstructure) is $[01\bar{1}]$, $[\bar{1}01]$, and $[1\bar{1}0]$. Note that this mode is independent of a particular superstructure. This motion does not carry a dipole moment and therefore does not directly affect the dielectric behavior. The T_{2u} mode was observed using hyper-Raman in various lead-free perovskites below 300 cm^{-1} (Ref. 25) in close agreement with theoretical calculations.[26]

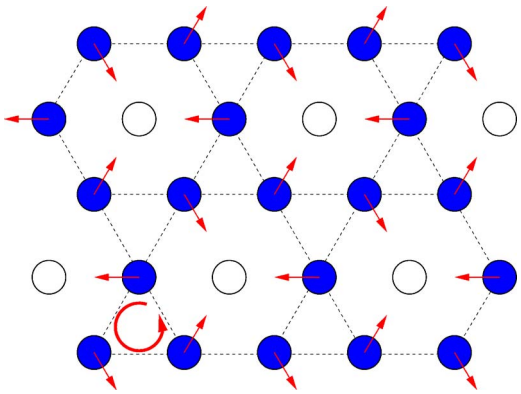

FIG. 4. (Color online) Vibrational displacements for the T_{2u} mode along (111) within the (111) plane (filled circles: oxygen atoms; open circles: lead atoms; arrows: displacement vectors). The rotation of the oxygen triangles is indicated by the rounded arrow.

The condensation of the transverse ferroelectric T_{1u} mode along (001) describes many features of the cubic-to-tetragonal phase transition in the end member PT, although strong indications for an order-disorder type of transition have been found as well.[27] The tetragonal lattice strain in PT is among the largest known in ferroelectrics.[2] This strain results from a strong coupling with the T_{1u} mode. PMN-rich compositions at low temperatures show comparably small rhombohedral strain.[7]

Beside the frequency of a vibrational mode, it is also described by its linewidth and mode strength. The linewidth Γ and the mode strength of the lower frequency mode are relatively constant above 650 K with Γ between 15 and 20 cm^{-1} and a maximum value of 26 cm^{-1} at 623 K. If this mode were of T_{1u} symmetry, the decreasing mode frequency would lead to an additional increase in the dielectric constant, which is not observed. Also, the observation that this mode does not couple to the central peak, while the other mode does, indicates that these two modes have different symmetries. We therefore follow that the lower frequency mode is

of T_{2u} symmetry. This interpretation is consistent with the observation that lead is offcentered along [001], but an additional soft-mode was found along [111].[6] The correlation between the observed softening at 571 K and T_d suggests that the origin of the deviation from linear high temperature behavior originates in the T_{2u} mode. Since the T_{2u} mode along (111) is hardly affected by the B-site cations, a Burns temperature independent on composition is expected. Observations on different compositions support this statement.[8,21] Also consistent with our interpretation, vibrational frequencies around 40 cm^{-1} have been assigned to Pb-O stretch modes.[28] Recent diffuse x-ray studies by Xu *et al.* on a similar relaxor system PZN-PT revealed static displacement vectors along $\langle 110 \rangle$ directions. This observation is consistent with the oxygen displacements described by the T_{2u} mode along (111).[29]

The mode strength and its temperature dependence strongly suggest that the modes observed in the hyper-Raman spectrum are first order modes. Therefore the other mode is expected to be a transverse T_{1u} mode. In conventional Raman spectroscopy at lower temperatures, modes at similar frequencies have been observed and were also found to strongly couple to the central peak.[30,31] Far-IR spectra also revealed a soft-mode and a central peak component,[32] while especially at low frequencies the resolution of far-IR measurements is significantly lower compared to spectra presented here. The linewidth of the coupled mode increases with decreasing temperature, peaks around 553 K and decreases again on further cooling. A linear fit to the inverse linewidth data above 560 K intersects the zero line around 400 K (not shown). The mode strength increases with decreasing temperature by a factor of about 100, indicating that this mode is still active and strongly coupled to the central peak at temperatures below 513 K. The observed strong coupling to the central peak implies that this vibrational mode has significant order-disorder components consistent with the Pb-O bond distances showing large variations.[6,21,33] Using the Kramers-Kronig relationship with the fitted parameters, not including the lower frequency mode, satisfactorily describes the dielectric properties. Since mode strengths in hyper-Raman spectra do not necessarily reflect IR mode strengths this observation does not permit clear mode symmetry assignment.

IV. SUMMARY

From the high temperature behavior above 580 K a classical soft-mode driven phase transition would be expected at 571 K, where the frequency of the T_{2u} mode approaches zero. The observation of the two modes not hardening again at temperatures below 570 K is different from the classical picture of soft-mode driven phase transitions. It seems possible that the T_{2u} mode is geometrically frustrated and the resulting short-range order is not compatible with a ferroelectric mode along (001) leading to the observed dissipation of the T_{1u} mode. Further measurements on different compositions are needed to verify the proposed model and to obtain detailed information on the compositional dependence of the mode frequencies.

ACKNOWLEDGMENTS

We would like to thank Scott Wilson for help with the x-ray measurements and Jie Li for essential equipment and support.

*Electronic address: hhellwig@uiuc.edu

[1] S. W. Choi, T. R. Shrout, S. J. Jang, and A. S. Bhalla, Ferroelectrics **100**, 29 (1989).
[2] M. L. Lines and A. M. Glass, *Principles and Applications of Ferroelectrics and Related Materials* (Oxford University Press, Oxford, 1977).
[3] G. Shirane, J. D. Axe, J. Harada, and J. P. Remeika, Phys. Rev. B **2**, 155 (1970).
[4] G. Burns and B. A. Scott, Phys. Rev. B **7**, 3088 (1973).
[5] M. D. Fontana, H. Idrissi, G. E. Kugel, and K. Wojcik, J. Phys.: Condens. Matter **3**, 8695 (1991).
[6] B. Dkhil, J. M. Kiat, G. Calvarin, G. Baldinozzi, S. B. Vakhrushev, and E. Suard, Phys. Rev. B **65**, 024104 (2001).
[7] Z.-G. Ye, Y. Bing, J. Gao, A. A. Bokov, P. Stephens, B. Noheda, and G. Shirane, Phys. Rev. B **67**, 104104–1 (2003).
[8] O. Noblanc, P. Gaucher, and G. Calvarin, J. Appl. Phys. **79**, 4291 (1996).
[9] B. Noheda, D. E. Cox, G. Shirane, J. Gao, and Z. G. Ye, Phys. Rev. B **66**, 054104 (2002).
[10] G. Xu, D. Viehland, J. F. Li, P. M. Gehring, and G. Shirane, Phys. Rev. B **68**, 212410 (2003).
[11] A. Sehirlioglu, D. A. Payne, and P. D. Han, Phys. Rev. B **72**, 214110 (2005).
[12] A. Naberezhnov, S. Vakhrushev, B. Dorner, D. Strauch, and H. Moudden, Eur. Phys. J. B **11**, 13 (1999).
[13] S. Wakimoto, C. Stock, Z.-G. Ye, W. Chen, P. M. Gehring, and G. Shirane, Phys. Rev. B **66**, 224102 (2002).
[14] S. B. Vakhrushev and S. M. Shapiro, Phys. Rev. B **66**, 214101 (2002).
[15] S. N. Gvasaliya, B. Roessli, R. A. Cowley, P. Huber, and S. G. Lushnikov, J. Phys.: Condens. Matter **17**, 4343 (2005).
[16] V. N. Denisov, B. N. Mavrin, and V. B. Podobedov, Phys. Rep. **151**, 1 (1987).
[17] H. Hellwig, Appl. Phys. Lett. **87**, 051104 (2005).
[18] H. Hellwig, R. J. Hemley, and R. E. Cohen, AIP Conf. Proc. **677**, 65 (2003).
[19] R. K. Wehner and E. F. Steigmeier, RCA Rev. **36**, 70 (1975).
[20] G. Burns and F. H. Dacol, Phys. Rev. B **28**, R2527 (1983).
[21] P. Bonneau, P. Garnier, E. Husson, and A. Morell, Mater. Res. Bull. **24**, 201 (1989).
[22] H. Vogt, Phys. Rev. B **41**, 1184 (1990).
[23] K. Inoue, Ferroelectrics **52**, 253 (1983).
[24] P. K. Davies and M. A. Akbas, J. Phys. Chem. Solids **61**, 159 (2000).
[25] H. Vogt and H. Uwe, Phys. Rev. B **29**, 1030 (1984).
[26] H. Vogt, Phys. Rev. B **38**, 5699 (1988).

[27] N. Sicron, B. Ravel, Y. Yacoby, E. A. Stern, F. Dogan, and J. J. Rehr, Phys. Rev. B **50**, 13168 (1994).
[28] E. Husson, L. Abello, and A. Morell, Mater. Res. Bull. **25**, 539 (1990).
[29] G. Xu, Z. Zhong, H. Hiraka, and G. Shirane, Phys. Rev. B **70**, 174109 (2004).
[30] I. G. Siny, S. G. Lushnikov, R. S. Katiyar, and E. A. Rogacheva, Phys. Rev. B **56**, 7962 (1997).
[31] O. Svitelskiy, J. Toulouse, G. Yong, and Z.-G. Ye, Phys. Rev. B **68**, 104107 (2003).
[32] S. Kamba, E. Buixaderas, J. Petzelt, J. Fousek, J. Nosek, and P. Bridenbaugh, J. Appl. Phys. **93**, 933 (2003); J. Hlinka, T. Ostapchuk, D. Noujni, S. Kamba, and J. Petzelt, Phys. Rev. Lett. **96**, 027601 (2006).
[33] I.-K. Jeong, T. W. Darling, J. K. Lee, Th. Proffen, R. H. Heffner, J. S. Park, K. S. Hong, W. Dmowski, and T. Egami, Phys. Rev. Lett. **94**, 147602 (2005).